Identification of Membrane-Anchoring Domains of RLIP76 Using Deletion Mutant Analyses †

ARTICLE *in* BIOCHEMISTRY · JANUARY 2005

Impact Factor: 3.02 · DOI: 10.1021/bi0482811 · Source: PubMed

8 AUTHORS, INCLUDING:

Sushma Yadav
City of Hope National Medical Center
36 PUBLICATIONS **809** CITATIONS
SEE PROFILE

Jyotsana Singhal
City of Hope National Medical Center
56 PUBLICATIONS **1,138** CITATIONS
SEE PROFILE

Yogesh C Awasthi
University of North Texas HSC at Fort Worth
313 PUBLICATIONS **11,317** CITATIONS
SEE PROFILE

Sanjay Awasthi
Beckman Research Institute
208 PUBLICATIONS **6,595** CITATIONS
SEE PROFILE

Identification of Membrane-Anchoring Domains of RLIP76 Using Deletion Mutant Analyses†

Sushma Yadav,‡ Sharad S. Singhal,‡ Jyotsana Singhal,‡ Dilki Wickramarachchi,‡ Eugene Knutson,§ Thomas B. Albrecht,§ Yogesh C. Awasthi,|| and Sanjay Awasthi*,‡

Department of Chemistry and Biochemistry, University of Texas, Arlington, Texas 76019-0065, and Department of Microbiology and Immunology and Department of Human Biological Chemistry and Genetics, University of Texas Medical Branch, Galveston, Texas 77555-0645

Received August 10, 2004; Revised Manuscript Received October 4, 2004

ABSTRACT: RLIP76 (RALBP1) is a multifunctional transporter involved in signaling and transmembrane movement of solute allocrites, which include glutathione conjugates and several natural product antineoplastic agents [Awasthi, S., et al. (2000) *Biochemistry 39*, 9327−9334; (2001) *Biochemistry 40*, 4159−4168]. Our previous studies suggested that the membrane-anchoring domain resides in the N-terminus of RLIP76, despite the lack of identifiable membrane-spanning domains. Amino acid sequence analysis indicated that this region of RLIP76 contains sequences that are similar to those of vector peptides. We, therefore, have studied the effect of a series of deletion mutant proteins on hydrophobicity and transport activity. RLIP76 or one of its derived deletion mutants was expressed in *Escherichia coli*, and bacteria were lysed and extracted in buffer without or with the nonionic detergent polidocanol. The ratio of RLIP76 in the detergent/aqueous extracts was found to be 2.5 for the wild-type protein, but decreased to 0.7 in the mutant in which amino acids 154−219 were deleted. Deletion of only one segment of this region (amino acids 171−185) alone resulted in a significant decrease in this ratio to 1.0. For the mutants with deletions within the region from amino acid 154 to 219, loss of hydrophobicity correlated with less incorporation of mutants into artificial liposomes, and decreased transport activity toward doxorubicin and dinitrophenyl-*S*-glutathione. In contrast, deletion of one of the two ATP-binding sites (at amino acids 65−80 or 415−448) or both sites did not affect hydrophobicity but reduced or abrogated transport activity. NSCLC (H358) stably transfected with del171−185 and del154−219 showed that loss of these regions results in a decrease in the extent of membrane association of RLIP76. Confocal laser immunohistochemistry colocalized amino acids 171−185 with her2/neu on the cell surface. Depletion of wild-type RLIP76 using si-RNA directed to this region in cells transfected with del171−185 resulted in the loss of cell surface expression. These finding demonstrate that amino acids 171−185 constitute a cell surface epitope which is necessary for optimal transport of anthracycline and glutathione conjugates by RLIP76, and that this peptide could be a novel target for antineoplastic therapy.

RLIP76 (RALBP1),[1] originally cloned as Ral-binding protein, is shown to be a Ral-regulated multifunctional protein involved in multispecific transport of structurally unrelated amphiphilic xenobiotics as well as glutathione−electrophile conjugates (GS−E) formed from xenobiotics and an electrophilic byproduct of oxidative metabolism (*1*−*14*). It is capable of coupling ATP hydrolysis with the translocation of a broad range of structurally unrelated xeno- and endobiotics against the concentration gradient, and its ATPase activity is stimulated in the presence of its transport substrates (allocrites) (*14*−*21*). Other investigators have shown independently that RLIP76 is an integral component of complexes containing Ral, clathrin-adaptor protein AP2, POB1 (partner of RALBP1), and epsin which are involved in the clathrin-coated-pit-mediated receptor−ligand endocytosis, a mechanism for internalizing receptor−ligand pairs to shut off signaling (*22*−*25*). Phosphorylation of these proteins has been directly linked to signaling via epidermal growth factor receptor (EGFR), insulin, and transforming growth factor-β receptor (TGF-βR) (*22*). Taken together with results of our studies establishing the function of RLIP76 as a glutathione conjugate transporter, and our recent studies showing that POB1 specifically binds to and inhibits the transport function of RLIP76 (S. Awasthi et al., unpublished observations), a model has emerged which indicates a crucial role for the transport of endogenous glutathione conjugates such as leukotriene C4 (*26*) in the

† Supported in part by NIH Grants CA 77495 and CA 104661 (S.A.), NIH Grant ES 012171, and NIEHS Center Grant ES 00677 (Y.C.A.).

* To whom correspondence should be addressed: Department of Chemistry and Biochemistry, 502 Yates St., Science Hall #223, University of Texas, Arlington, TX 76019-0065. Phone: (817) 272-5444. Fax: (817) 272-3808. E-mail: sawasthi@uta.edu.

‡ University of Texas at Arlington.

§ Department of Microbiology and Immunology, University of Texas Medical Branch.

|| Department of Human Biological Chemistry and Genetics, University of Texas Medical Branch.

[1] Abbreviations: aa, amino acid(s); RLIP76 (RALBP1), ral-interacting protein; DOX, doxorubicin; GSH, glutathione; GS−E, glutathione−electrophile conjugate; DNP-SG, dinitrophenyl-*S*-glutathione; POB1, partner of RALBP1; NSCLC, non-small cell lung cancer.

10.1021/bi0482811 CCC: $27.50
Published on Web 12/04/2004

process of clathrin-dependent receptor−ligand pair endocytosis. Even though multiple membrane-associated functions of RLIP76, including ATP-dependent transport (*13*, *14*), its role as an effector protein in signaling pathways, mitosis, membrane ruffling, and receptor-mediated endocytosis (*4*, *9*, *22*−*25*), along with evidence published by us (*14*) and others (*8*) indicate that RLIP76 is a membrane-associated protein, definitive proof for this assertion has been lacking.

Our previous results have shown that the N-terminus of RLIP76 (N-RLIP$^{1-367}$) is membrane-associated and can be extracted only with the detergent. In contrast, the C-terminus of RLIP76 (RLIP$^{410-655}$) was found to be in both the aqueous and the detergent extracts (*1*, *14*). Approximately 80% of RLIP76 expressed in *Escherichia coli* was found in the particulate fraction in absence of the detergent but could be extracted with polidocanol (*1*, *13*, *14*). Earlier studies also suggest the association of RLIP76 and its mouse and rat homologues RIP1 and RalBP1 with membranes. It has been shown that activated Ral, one of the important factors in signal transduction, translocates RLIP76 to the cell membrane inhibiting the GAP activity of this protein toward Rac1 and cdc42 (*27*, *28*). The rat and mouse homologues of RLIP76, RalBP1 and RIP1, respectively, appear to be membrane-associated in our studies (*1*, *29*−*31*) as well as studies by other investigators (*7*, *8*). These results suggested that RLIP76 contains sequences that are responsible for anchoring the protein with the membrane. Indeed, our immunohistochemistry and flow cytometry studies have showed specific cell surface recognition of ligand(s) by anti-RLIP76 antibody in human lung cancer cell lines, suggesting the existence of transmembrane regions (*12*).

Sequence analysis of RLIP76 does not reveal classical transmembrane helices, but hydropathy plot studies have shown two regions of relatively high hydrophobicity, which could potentially reside within the membrane (*1*). Amino acid sequence analysis indicated that RLIP76 has sequences with some degree of homology to the vector peptides such as penetratin, Tat, and MAP (Figure 1A). Vector peptides are known to reside in membranes and are capable of being internalized in most cell types. These peptides could translocate into the cells by endocytosis and direct transport through the cell membrane (*32*, *33*). Since vector peptides can traverse membranes, we reasoned that amino acid sequences adjacent to vector peptide-homologous sequences could be translocated to the outer layer of the plasma lemma. To test this hypothesis, we determined the detergent solubility, transport activity, and membrane distribution of a series of deletion mutants (Figure 1E) of RLIP76. Our studies indicate that amino acids 171−185 promote membrane association, and that this peptide is displayed on the cell surface.

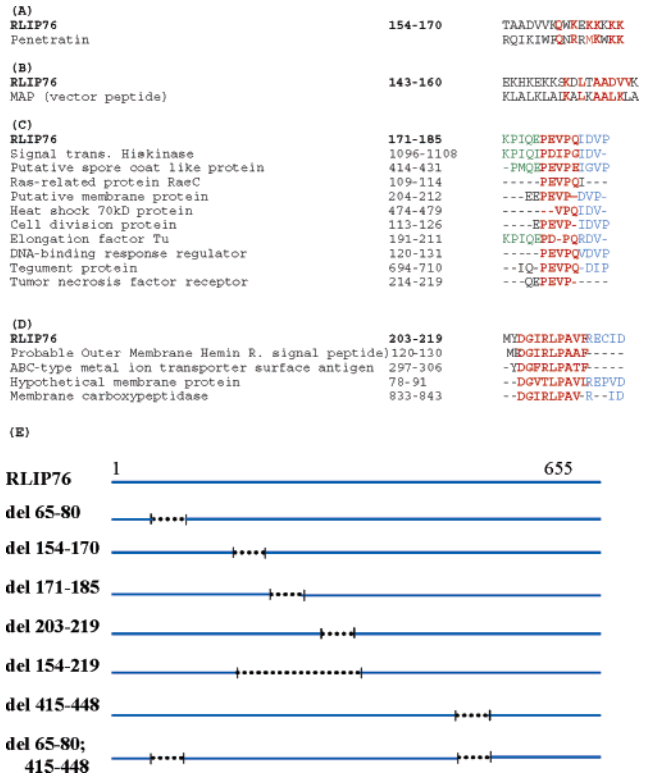

FIGURE 1: Sequence homology of regions of RLIP76: with vector peptides penetratin (A) and MAP (B) and with other proteins (C and D). (E) Schematic representation of various deletion mutants of RLIP76.

EXPERIMENTAL PROCEDURES

Materials. RPMI-1640 medium, phosphate-buffered saline (PBS), a penicillin/streptomycin solution (P/S), fetal bovine serum (FBS), trypsin-EDTA, trypan blue, and agarose were purchased from Gibco BRL Inc. (Grand Island, NY). ATP, β-mercaptoethanol (BME), phenylmethanesulfonyl fluoride (PMSF), polidocanol, 3-(4,5-dimethylthiazol-2-yl)-2,5-diphenyltetrazolium bromide (MTT), DMSO, L-glutamine, HEPES, sodium pyruvate, glucose, sodium bicarbonate, cholesterol, soybean asolectin, kanamycin, isopropyl β-D-thiogalactopyranoside (IPTG), and G418 (Geneticin) were purchased from Sigma Chemical Co. (St. Louis, MO). Doxorubicin (adriamycin) was obtained from Adria Laboratories (Columbus, OH). DE-52 (diethylaminoethylcellulose) anion exchanger was purchased from Whatman International Ltd. (Maidstone, England). Bio-Beads (SM-2 adsorbent) and Chelex-100 resin were purchased from Bio-Rad Laboratories (Hercules, CA). Tryptone and yeast extract for preparing culture media were purchased from Difco Laboratories (Detroit, MI). PCR purification, gel extraction, pDNA purification, transfection reagent selector, transmessenger transfection reagent, and one-step RT-PCR kits were purchased from Qiagen (Valencia, CA). [γ-^{32}P]ATP (3000 Ci/mmol) was purchased from Pharmacia Biotech (Piscataway, NJ). [^{14}C]DOX (specific activity of 57 mCi/mmol) was purchased from Amersham Corp. (Arlington Heights, IL). Bacterial strains [DH5α and BL21(DE3)] were purchased from Invitrogen Life Technology (Carlsbad, CA). pET30a(+), the T7 promoter-based expression vector, was purchased from Novagen, Inc. (Madison, WI). Restriction enzymes, thermophilic DNA polymerase (Vent polymerase), and DNA ligase were from New England Biolabs (Beverly, MA). dNTPs were from Applied Biosystems (Foster City, CA). HPLC-grade oligonucleotides were synthesized by Biosynthesis, Inc. (Lewisville, TX). Polyclonal rabbit anti-human rec-RLIP76 IgG and preimmune IgG were prepared and purified as described previously (*13*, *14*). Anti-171−185 siRNA was from Dharmacon Research (Lafayette, CO). Polyclonal antibodies against various regions of RLIP76 were custom-made and purchased from Alpha Diagnostics (San Antonio, TX). These peptide antibodies as well as preimmune serum were purified

by DE-52 anion exchange chromatography, followed by protein A−Sepharose affinity chromatography to obtain pure IgG fractions. The immunoreactivity and specificity of these peptides using their respective purified IgG were checked by dot blot analyses. Human herceptin (her2/neu) antibodies were purchased from Genentech, Inc. (South San Francisco, CA). Human IgG was purchased from Baxter Healthcare Corp. FITC-conjugated goat anti-rabbit and FITC-conjugated goat anti-human antibodies were purchased from Vector Laboratories, Inc. (Burlingame, CA). Rhodamine red x-conjugated goat anti-rabbit antibodies were purchased from Jackson Immuno Research Laboratories (West Grove, PA).

Cloning and Prokaryotic Expression of RLIP76. Wild-type construct pET30a(+)/RLIP76 was available in our laboratory. It was amplified from the RLIP76 λgt11 cDNA clone as described previously (*13*). PCR primers were designed to introduce a BamHI restriction site immediately upstream of the initiator codon, and an XhoI site immediately downstream of the stop codon of the RLIP76 open reading frame. The PCR product was cloned into vector pET30a(+) previously cut with the same enzymes, creating pET30a(+)/RLIP76 free of extraneous sequences.

In Vitro Site-Directed Mutagenesis. A series of deletion mutants of RLIP76 were made by PCR-based site-directed mutagenesis using a clone of the full-length RLIP76 in the pET30a(+) expression vector as a template, upstream primer 5′-GGCGGATCCATGACTGAGTGCTTCCT (BamHI restriction site underlined), and downstream primer 5′-CCGCTCGAGTAGATGGACGTCTCCTTCCTATCCC (XhoI restriction site underlined). The mutagenic primers were as follows: aa 203−219 deletion (del203−219), 5′-GTAGAGAGGACCATGGTAGAGAAGTATGGC-3′ (with its reverse complement); aa 154−170 deletion (del154−170), 5′-GAAGAAGTCAAAAGACAAGCCAATTCAGGAG (with its reverse complement); aa 171−185 deletion (del171−185), 5′-GAAGAAAAAGAAACTCAAACCCATTTTT-3′ (with its reverse complement); aa 154−219 deletion (del154−219), 5′-GAAGAAGTCAAAAGACGTAGAGAAGTATGGC-3′ and its reverse complement; aa 415−448 deletion (del415−448), 5′-GAATTGTTTACATCGACAGGAGTGTGAAACC (with its reverse complement); and aa 65−80 deletion (del65−80), 5′-GTGTCTGATGATAGGACTGAAGGC-TATG 3′ and its reverse complement.

In two separate reactions, the two "halves" of the regions to be deleted were amplified by PCR under the following conditions: 500 ng of DNA template, primers (30 pmol each), 2.5 μM dNTPs, 1× thermopol buffer, 1× BSA, and 2.5 units of Vent polymerase. PCR cycles were as follows: 94 °C for 5 min followed by 30 cycles of 30 s at 94 °C, 30 s at 60 °C, and 1 min at 72 °C and a final extension of 7 min at 72 °C. The PCR products were gel purified using the Qiagen gel purification kit, and the purified products of both PCRs in a 1:1 molar ratio were extended at 94 °C for 5 min followed by 12 cycles of 30 s at 94 °C, 1 min at 50 °C, and 2 min at 72 °C and a final extension of 7 min at 72 °C. The PCR products were purified by using the Qiagen PCR purification kit and digested with BamHI−XhoI restriction enzymes.

The BamHI−XhoI-cleaved PCR products were gel purified and ligated into pET30a(+) previously digested with the same restriction enzymes. The ligated products were cloned and the colonies screened for mutation, and plasmid DNA was purified from the overnight culture of a single colony using the Qiagen DNA purification kit. Techniques for restriction enzyme digestion, ligation, transformation, and other standard molecular biology manipulations were based on methods described by Sambrook et al. (*34*). The authenticity of the mutation and the absence of other fortuitous mutations were confirmed by DNA sequencing for each of the deletion mutants.

Distribution of RLIP76 in the Cytosol and Membrane of E. coli Expressing Wild-Type and Mutant RLIP76. Following verification of the desired deletion, the pET30a(+) plasmid containing the full-length RLIP76 (wt-RLIP76) and its deletion mutants (del203−219, del154−170, del171−185, del154−219, del65−80, del415−448, and del65−80;415−448) were used to transform *E. coli* strain BL21(DE3) in which the expression of the recombinant protein is under the control of the lac UV5 promoter. Single bacterial colonies were inoculated in LB medium containing 30 μg/mL kanamycin, and the bacteria were grown at 37 °C overnight with shaking at 225 rpm. The overnight culture was diluted 100 times and grown in LB containing the same antibiotic at 37 °C until the OD_{600} reached 0.6. This was followed by addition of 0.4 mM IPTG to induce protein expression and incubation at 37 °C overnight. The bacterial pellet collected by centrifugation at 1400*g* was lysed in lysis buffer [10 mM Tris-HCl (pH 7.4) containing 1.4 mM β-mercaptoethanol, 100 μM EDTA, 50 μM butylated hydroxytoluene (BHT), and 100 μM PMSF], sonicated for 30 s at 50 W (three times), and incubated for 4 h at 4 °C with gentle shaking. After incubation, the mixture was centrifuged at 105000*g* for 1 h at 4 °C and the supernatant was termed the cytosol fraction. The pellet was resuspended in lysis buffer containing 1% polidocanol ($C_{12}E_9$). To facilitate the extraction of rec-RLIP76 and its various deletion mutants, lysates were sonicated for 30 s at 50 W (three times) and incubated for 4 h at 4 °C with gentle shaking. After incubation, the reaction mixture was centrifuged at 105000*g* for 1 h at 4 °C, and the supernatant fraction thus obtained was termed membrane fraction. Since polidocanol interfered with Bradford's reagent, the protein concentration was estimated by the method of Minamide and Bamburg (*35*).

SDS−PAGE and Western Blot Analyses. Each protein (100 μg) was subjected to SDS−PAGE, and Western blot analyses of both the cytosol and membrane fraction of the protein were carried out by transferring the resolved protein on 12.5% acrylamide gels to a nitrocellulose membrane using the method of Towbin et al. (*36*). The membranes were then incubated with anti-RLIP76 antibodies as the primary antibody followed by horseradish peroxidase-conjugated goat anti-rabbit IgG as a secondary antibody. The blots were developed using 4-chloro-1-naphthol, and developed bands were quantified by scanning densitometry.

Purification of RLIP76 and Its Various Deletion Mutants by DNP-SG Affinity Chromatography. We have shown that DNP-SG affinity resin prepared as previously described (*13*) can be used to purify RLIP76 to near homogeneity from the total bacterial extracts of *E. coli*. It was determined that the introduction of deletions specified above in wild-type RLIP76 did not affect the affinity of the protein with DNP-SG, and all the deletion mutants could be purified by DNP-SG affinity chromatography. Therefore, *E. coli* heterologously overexpressing RLIP76 or its deletion mutants was lysed in the

presence of 1% (w/v) $C_{12}E_9$ in lysis buffer and RLIP76, or its deletion mutants were purified by DNP-SG affinity chromatography according to the method described previously (*13*). The purity of these fractions was ascertained by SDS−PAGE, Western blot, and amino acid composition analysis as described previously (*13*). All purification steps were carried out at 4 °C unless otherwise specified.

Reconstitution of Purified RLIP76 and Its Deletion Mutants into Artificial Liposomes and Transport Studies. Functional reconstitution of purified RLIP76 from *E. coli* for transport studies was performed as described previously (*13*, *15*). The degree of incorporation of the wild-type and mutant RLIP76 into artificial liposomes was assessed by measuring the amount of RLIP76 in the 105000*g* pellet and supernatant of the prepared liposomes by an ELISA using anti-RLIP76 antibodies. Assessment of the transport of DOX in these reconstituted liposomes was performed as described previously (*13*, *14*), and the rate of ATP-dependent uptake of [^{14}C]DOX (specific activity of 8.4×10^4 cpm/nmol) was determined by subtracting the radioactivity (counts per minute) of the control without ATP from that of the experimental containing ATP. The rate of transport of DOX was calculated in terms of picomoles per minute per milligram of protein. The rate of transport of [^{3}H]DNP-SG (specific activity of 3.2×10^3 cpm/nmol) was measured using a similar protocol described previously (*13*, *14*).

Cell Lines and Cultures. Human NSCLC line H358 (bronchioalveolar) was used in these studies. It was a kind gift from A. F. Gazdar at the University of Texas Southwestern Medical Center (Dallas, TX).

Cells were cultured at 37 °C in a humidified atmosphere of 5% CO_2 in RPMI-1640 medium supplemented with 10% (v/v) heat-inactivated FBS, 1% (v/v) P/S solution, 2 mM L-glutamine, 10 mM HEPES, 1 mM sodium pyruvate, 4.5 g/L glucose, and 1.5 g/L sodium bicarbonate.

Eukaryotic Expression of RLIP76 and Its Deletion Mutants. H358 cells were transfected with the eukaryotic expression vector alone (pcDNA-3.1), pcDNA-3.1/RLIP76, and pcDNA-3.1/del171−185 using the Effectene Transfection Reagent kit (Qiagen). Stable transfectants were selected in the presence of 600 μg/mL G418 for 2 weeks. Several G418-resistant stable clones were selected for further characterization and were maintained in medium containing 300 μg/mL G418. A single clonal stable transfectant was established by sequential dilution into a 96-well plate, so only a single cell was seeded in each well. Expression of RLIP76 mRNA in lung cancer cell lines was evaluated by RT-PCR analysis. The RNA was prepared with the RNeasy kit (Qiagen) and quantified by measuring the optical density at 260 and 280 nm. For electrophoresis, 2 μg of RNA was denatured in 50% formamide containing 2.2 M formaldehyde at 65 °C for 10 min, chilled in ice for 5 min, and subsequently subjected to 1% agarose gel electrophoresis in MOPS-formaldehyde buffer for 3 h at 50 V. RT-PCR was performed on mRNA isolated from control, vector alone, RLIP76, and del171−185 transfected clones. RLIP76 gene-specific primers [1495−1514 bp (upstream primer) and 1948−1968 bp (downstream primer)] were used for RT-PCR. The one-step RT-PCR kit was used according to the manufacturer's instructions (Qiagen).

Distribution of RLIP76 and Its Various Deletion Mutants in Detergent and Aqueous Fractions in NSCLC. Cells were pelleted at 700*g*, solubilized in lysis buffer [10 mM Tris-HCl (pH 7.4) containing 1.4 mM β-mercaptoethanol, 100 μM EDTA, 50 μM BHT, and 100 μM PMSF], sonicated for 30 s at 50 W (three times), and incubated for 4 h at 4 °C with gentle shaking. After incubation, the reaction mixture was centrifuged at 105000*g* for 1 h at 4 °C, and the supernatant containing the cytosol fraction was collected. To extract the membrane protein, the pellet was resuspended in lysis buffer containing 1% polidocanol ($C_{12}E_9$), sonicated for 30 s at 50 W (three times), and incubated for 4 h at 4 °C with gentle shaking. After incubation, the reaction mixture was centrifuged at 105000*g* for 1 h at 4 °C, and the supernatant containing the solubilized membrane fraction was collected.

RLIP76 siRNA Preparation. The region spanning amino acid residues 171−185 (nucleotides 510−555 starting from the 1 AUG codon in the open reading frame) in the N-terminal region of RLIP76 was chosen as the target region for designing siRNA. We searched for a 23-nucleotide sequence motif, AA(N19)TT or NA(N21) (N, any nucleotide), and selected hits with approximately 50% GC content. The sequence of sense siRNA corresponds to N21. We converted the 3′-end of the sense siRNA to TT. The rationale for this sequence conversion was to generate a symmetric duplex with respect to the sequence composition of sense and antisense 3′-overhangs. The selected siRNA sequence was subjected to blast-search (NCBI database) against EST libraries, to ensure that only one gene was targeted. The chemically synthesized siRNA duplex in the 2′-deprotected and desalted forms was purchased from Dharmacon. A 23-nucleotide scrambled siRNA duplex was used as a control. The scrambled siRNA sequence was not homologous with RLIP76 mRNA in a blast-search against RLIP76. The targeted cDNA sequence (AAGAAAAAGCCAATTCAGGAGCC) corresponds to nucleotides 508−528. The corresponding sense and antisense siRNA sequences were GAAAAAGCCAAUUCAGGAGCCdTdT and GGCUCCUGAAUUGGCUUUUUCdTdT, respectively. The sequences of the scrambled siRNA in the sense and antisense directions were GUAACUGCAACGAUUUCGAUGdTdT and CAUCGAAAUCGUUGCAGUUACdTdT, respectively. Transfection of siRNA duplexes was performed using the transmessenger transfection reagent kit (Qiagen) and assayed for expression 24 h after transfection.

Effect of RLIP76 siRNA on Protein Expression. Cells (3×10^6) were placed in six-well plates and, after preincubation for 24 h in the medium, were incubated with RLIP76 or scrambled siRNA in transmessenger transfection reagent for 3 h. After incubation, excess siRNA was washed off with PBS and medium was added. Cells were pelleted at 700*g* and solubilized in lysis buffer [10 mM Tris-HCl (pH 7.4) containing 1.4 mM β-mercaptoethanol, 100 μM EDTA, 50 μM BHT, 100 μM PMSF, and 1% polidocanol]. The mixture was sonicated for 30 s at 50 W (three times) and incubated for 4 h at 4 °C with gentle shaking. After incubation, the mixture was centrifuged at 105000*g* for 1 h at 4 °C, and the supernatant containing both the cytosolic proteins and solubilized membrane proteins was collected and used for SDS−PAGE. Aliquots of this supernatant containing 100 μg of protein were applied to SDS−PAGE; Western blot analysis was performed according to the method of Towbin et al. (*36*) using anti-RLIP76 IgG as well as IgG against

peptide 171−185, and the bands were quantified by scanning densitometry using an Alpha Innotech Imager.

Immunofluorescence and Confocal Laser Scanning Microscopy. For immunohistochemical localization of RLIP76 in cancer cells, aliquots of del171−185-transfected H358 cells (approximately 1×10^6 cells) were grown on sterilized glass coverslips in a 12-well plate. After 24 h, the coverslips were blocked with 10% goat serum for 60 min at room temperature, and anti-RLIP76 IgG was added at a concentration of 100 μg/mL and incubated for 2 h at room temperature in a humidified chamber. After the mixture had been washed with PBS four or five times, FITC-conjugated secondary antibodies were added and incubated for 1 h at room temperature in a humidified chamber followed by washing with PBS four or five times. Finally, coverslips were removed and dried in air and mounted on slides upside down with Vectashield mounting medium for fluorescence (Vector Laboratories). Picture were taken using a Zeiss LSM 510META laser scanning fluorescence microscope.

Immunohistochemical Localization of RLIP76. Immunohistochemical localization of RLIP76 was performed on H358 cells transfected with del171−185 by the method described previously with slight modifications (*12*). Transfected cells were grown on coverslips. Nonspecific antibody interactions were minimized by pretreating cells with 10% goat serum in TBS for 60 min at room temperature. The cells were incubated with primary antibodies, anti-RLIP76 IgG, anti-del171−185 IgG, anti-her2/neu IgG, or preimmune IgG for 2 h at room temperature in a humidified chamber. After the primary antibody had been washed off with PBS (10 times, 3 min each), rhodamine red-x-conjugated goat anti-rabbit and fluorescein isothiocyanate (FITC)-conjugated goat anti-human IgG (1:50 dilution in PBS) as secondary antibodies for RLIP76 and Herceptin, respectively, were added and incubated for 1 h at room temperature in a humidified chamber. The unbound secondary antibodies were removed by washing with PBS (10 times, 3 min each), and coverslips were air-dried and mounted on the slides with Vectashield mounting medium for fluorescence (Vector Laboratories). Slides were photographed at 400× magnifications using a LEICA DMLB fluorescence microscope. Photographs were taken with 1 s integration.

Immunofluorescence studies with cells treated with siRNA were also examined as described above. For determination of the effect of siRNA, del171−185-transfected H358 cells were grown on coverslips. After incubation for 24 h with medium, cells were incubated with RLIP76 or scrambled siRNA in transmessenger transfection reagent for 3 h. Cells were then washed with PBS, followed by incubation for 24 h at 37 °C in medium before immunohistochemical localization studies.

RESULTS

Effect of Various Deletions on the Detergent Solubility in Bacterial Expression of rec-RLIP76. Using the IBM Bioinformatics Group Multiple Sequence Alignment algorithm, we analyzed several selected short peptides from the N-terminus of RLIP76 for sequence similarity with antennapedia homeodomain homologous peptides (vector peptides) as well as other proteins, and selected three candidates, aa 154−170, 171−185, and 203−219. The peptide of aa 154−170 was similar to penetratin (Figure 1). The peptides of aa 171−185 and 203−219 were found in several membrane proteins, and the peptide of aa 203−219 was highly hydrophobic. We devised deletion mutants, one for each of the three selected peptides, and one covering all three (154−219). These mutants were cloned into prokaryotic expression vector pET30a(+) and expressed in *E. coli*. After induction with IPTG, bacteria were lysed, and the lysate was extracted with buffer without or with polidocanol, a nonionic detergent. Western blot analysis of these extracts (Figure 2) against anti-RLIP76 antibodies raised against purified recombinant full-length RLIP76 showed the same pattern of bands representing RLIP76 and its proteolytic degradation products as we have previously reported (*13*, *14*). The band at ∼95 kDa representing full-length RLIP76 was quantified by scanning densitometry from three separate experiments, and a ratio of detergent to aqueous soluble protein was calculated (Figure 2). For wild-type RLIP76, this ratio was found to be 2.5, and for the deletion mutant del203−219, this ratio was not affected (2.6). For the del154−170 mutant, this ratio was reduced slightly (2.0) but significantly ($p < 0.05$). In contrast, the del171−185 mutant had a much stronger effect, where the ratio was reduced to 1.0. This ratio was further reduced to 0.7 for the del154−219 mutant. As controls, we also analyzed the effect on the detergent to aqueous extraction ratio of deletion mutants containing one or both of the ATP binding sites, aa 65−80 and 415−448 (*14*). The ratios of detergent to aqueous fraction of these mutants were same as that for wt-RLIP76, indicating that the observed effect of deletion of aa 154−219 was a specific effect, rather than simply due to a nonspecific effect of any deletion. These results are consistent with results of our previous studies on recovery of the N-terminal (1−367) and C-terminal (410−655) peptides of RLIP76 from bacterial extracts with or without detergent (*14*) and indicate that aa 154−219 of RLIP76 significantly affect its partitioning between the

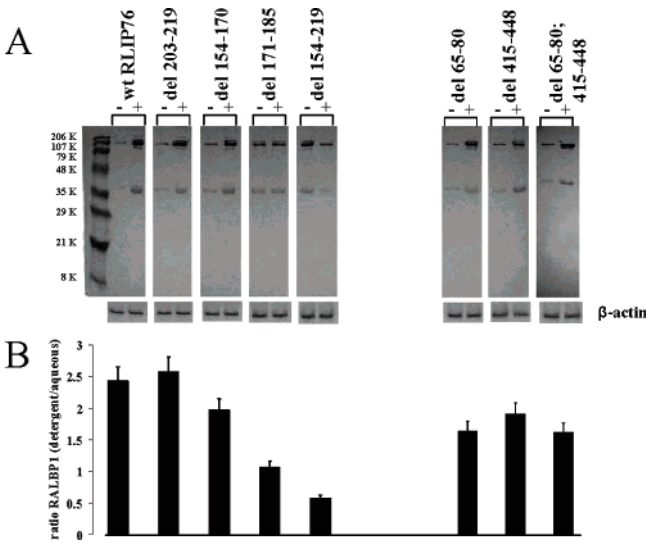

FIGURE 2: Partitioning of RLIP76 in detergent and aqueous fractions of the extracts of *E. coli* transformed with wt-RLIP76 and its deletion mutants. (A) The protein (100 μg each) from the lysates of *E. coli* prepared without and with 1% $C_{12}E_9$ was analyzed by Western blot analyses using anti-RLIP76 antibodies. β-Actin expression was used as an internal control. Peptide bands in Western blots were quantitated by scanning densitometry (B). In various lanes, − and + indicate the sample extracted without and with 1% polidocanol, respectively. Details are given in the text.

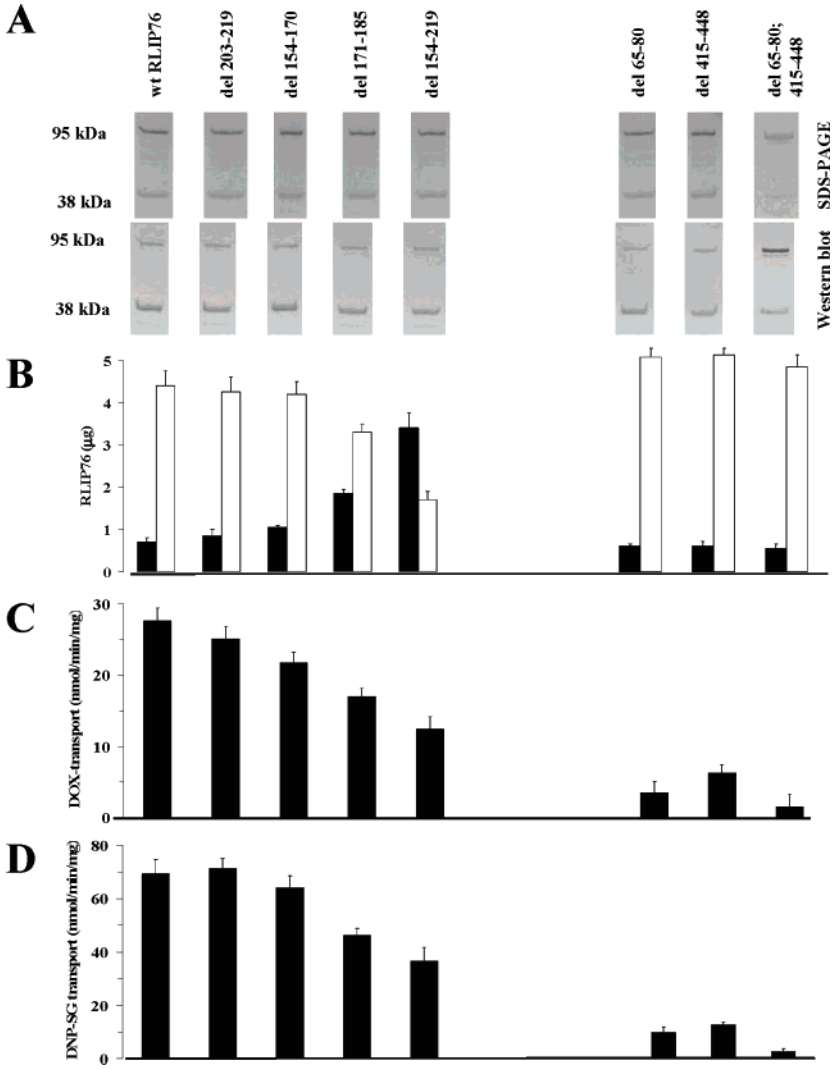

FIGURE 3: SDS−PAGE and Western blot analyses of rec-RLIP76 and its various deletion mutants used for transport studies. (A) The purified protein (10 μg) was subjected to SDS−PAGE, stained with Coomassie Brilliant Blue R-250, and subjected to Western blot analyses using full-length anti-RLIP76 antibodies. (B) The effect of deletion mutations on the incorporation of purified RLIP76 into artificial liposomes was assessed by measuring the amount of RLIP76 (using an ELISA with anti-RLIP76 IgG as the primary antibody) in the supernatant (black bars) and pellet (white bars) after 104000*g* centrifugation of the prepared proteoliposomes. For these studies, aliquots of proteoliposomes containing 7 μg of protein were subjected to ultracentrifugation. ATP-dependent transport of DOX (C) and DNP-SG (D) by proteoliposomes reconstituted with purified rec-RLIP76 and its various deletion mutants. The bar graphs in panels C and D represent transport activity of the corresponding protein in panel A. Purified proteins from transformed *E. coli* were reconstituted into artificial liposomes as described in Experimental Procedures. Control liposomes were prepared using equal amounts of protein from the extracts of noninduced *E. coli*. Transport assays were performed using a 96-well plate filtration device (*14*). Reaction mixtures containing reconstituted liposomes or proteoliposomes (250 ng of protein) were incubated with [^{14}C]DOX or [^{3}H]DNP-SG for 5 min at 37 °C. The transport reaction was started by addition of buffer without or with 4 mM ATP. The final concentrations of DNP-SG and DOX were 100 and 3.6 μM, respectively. Transport was assessed for 5 min at 37 °C, after which the reaction mixture was filtered through a 0.45 μm membrane in the Millipore 96-well plate manifold. The level of background binding of [^{14}C]DOX or [^{3}H]DNP-SG to the filter membrane was estimated by omitting liposomes from the transport reaction mixtures. The values for ATP-dependent transport presented in the bar graphs represent means ± the standard deviation (n = 12).

cytosol and membranes and that a majority of this effect is conferred by aa 171−185.

Purification of wt-RLIP76 and Its Deletion Mutants. To study the effect of these deletions on the transport activity of RLIP76, each of the deletion mutants was purified by established dinitrophenyl-*S*-glutathione/ATP affinity chromatography which we have shown previously to yield apparently homogeneous RLIP76 (*13*). During the affinity purifications, each of the deletion mutants was obtained in a similar yield, indicating that the deletions did not affect binding of the mutants to the DNP-SG affinity resin. The purity of RLIP76 and its mutants used for reconstitution in artificial asolectin liposomes to determine transport activity was established by SDS−PAGE and Western blot analyses. Results presented in Figure 3A showed the presence of only two major bands, one at ~95 kDa representing full-length RLIP76 and the other near 38 kDa representing a C-terminal fragment beginning at aa 424, as previously observed with homogeneous preparations of RLIP76 due to its facile degradation (*13*). Western blot analysis revealed that both bands were recognized by anti-RLIP76 IgG, indicating that RLIP76 and its deletion mutants reconstituted in liposomes for transport measurements were free from any contaminating protein.

Effect of Deletions on Transport Properties of RLIP76. Purified full-length RLIP76 and its deletion mutants were

reconstituted into proteoliposomes (*13*, *14*). The effect of deletion mutants on the efficiency of incorporation of RLIP76 into proteoliposomes was determined by quantifying RLIP76 immunologically in 104000*g* pellets and supernatants of aliquots of reconstituted proteoliposomes (Figure 3B). Results of these studies showed that the vast majority (87%) of total wild-type RLIP76 was found in the pellet fraction, incorporated into the proteoliposomes. Whereas deletion of aa 203−219 or 154−170 decreased the level of incorporation only slightly (to 83 or 80%, respectively), deletion of aa 171−185 had a significantly greater effect on incorporation of the protein into proteoliposomes (64%). Deletion of the entire region from aa 154 to 219 caused a more significant effect, with only 33% of the total protein found incorporated into the proteoliposomes. Deletions affecting the ATP-binding sites had no significant effect on the amount of protein incorporated into the proteoliposomes. These results suggested that aa 154−219 were an important determinant of membrane insertion. The effect of these deletion mutations was also assessed with respect to ATP-dependent transport of DOX and DNP-SG. Results presented in panels C and D of Figure 3 indicate that the DOX and DNP-SG transport activity of del203−219 was not significantly different from that of wild-type RLIP76, and a small but significant decrease (21%) in DOX transport activity was seen for the del154−170 (27.6 and 21.7 nmol min^{-1} mg^{-1} for full-length RLIP76 and the deletion mutant, respectively; $p < 0.05$). A similar reduction was seen in the transport activity of this mutant for DNP-SG transport. Deletion of aa 171−185 resulted in an approximately 40% loss of transport activity for DOX and a similar loss (35%) in transport activity for DNP-SG. Deletion of the entire region of aa 154−219 resulted in a further significant loss (50%) of transport activity for both DOX and DNP-SG. Deletion of the ATP-binding sites, which did not affect partitioning in detergent, affected DOX and DNP-SG transport differentially as shown previously (*14*). The deletion mutants, aa 65−80 and 415−448, had only ∼13 and ∼23% residual DOX transport activity, respectively, as compared to full-length RLIP76 (Figure 3C). Transport activity of these mutants for DNP-SG was also decreased to a similar extent (Figure 3D). Deletion of both ATP-binding sites resulted in near abrogation of transport for both DOX and DNP-SG [2 and 3% of the control as well as DOX- or DNP-SG-stimulated ATPase activity of RLIP76 (*14*)]. These results further confirmed ATP dependence of the transport as shown in our previous studies (*13*, *14*). Since our results show that ATP-binding site deletions did not affect partitioning of the mutants between the cytosol and membrane (Figure 2), these results also suggested that the observed decrease in the transport activity of the deletion mutant aa 154−219 (Figure 3C,D) resulted due to loss of its association with the membrane as indicated by its weakened partitioning in the membrane for action.

Effect of Deletions of aa 171−185 and 154−219 on Partitioning of RLIP76 between the Membrane and Cytosol in Eukaryotes .H358 cells were transfected with the empty pcDNA3.1 vector or the vector containing either full-length RLIP76 or its mutants (del171−185 or del154−219). Cells were sonicated in buffer without or with polidocanol, and equal protein aliquots of extracts were analyzed by Western blots. Similar to that observed in the prokaryotic cells, the membrane association of RLIP76 was also significantly

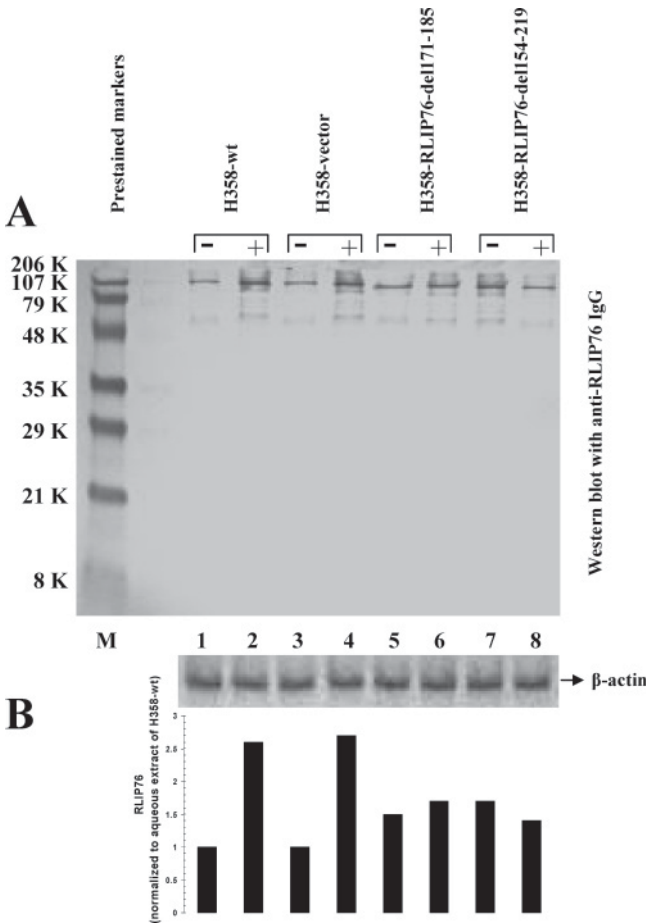

FIGURE 4: Distribution of RLIP76 and its various deletion mutants in the detergent and aqueous fractions in NSCLC. (A) The protein (100 μg each) from the aliquots of cells without (cytosol) and with 1% $C_{12}E_9$ (membrane) was analyzed by Western blot analyses using anti-RLIP76 antibodies: lane M, molecular mass markers; lanes 1 and 2, protein from the cytosol and membrane fraction, respectively, of the control H358 (NSCLC) cells; lanes 3 and 4, protein from the cytosol and membrane fraction, respectively, of H358 transfected with vector pcDNA3.1; lanes 5 and 6, protein from the cytosol and membrane fraction, respectively, of H358 transfected with del171−185; and lanes 7 and 8, protein from the cytosol and membrane fraction, respectively, of H358 transfected with del154−219. β-Actin expression was used as an internal control. Sample in lanes marked with a − were extracted without detergent and with a + with detergent. (B) Bar graph representing the quantification of the protein bands from the Western blots by scanning densitometry.

inhibited in these cells transfected with both deletion mutants (Figure 4). These findings indicate that aa 154−219 are a determinant of the membrane association of RLIP76, and it is independent of whether the protein is expressed in eukaryotes or prokaryotes.

Membrane Localization of RLIP76. Immunohistochemistry studies using anti-RLIP76 antibodies raised against full-length RLIP76 were performed with live, unfixed H358 wild-type cells and examined by confocal laser microscopy, which revealed a staining pattern consistent with cell surface recognition (Figure 5). In additional studies, we examined colocalization of RLIP76 with another protein, her2/neu, known to have a cell surface domain. The anti-RLIP76 antibody was detected using a rhodamine red-x-conjugated secondary antibody and anti-her2/neu antibody using an FITC-tagged secondary antibody. Cell surface epitopes were recognized by both anti-RLIP76 (red fluorescence, Figure

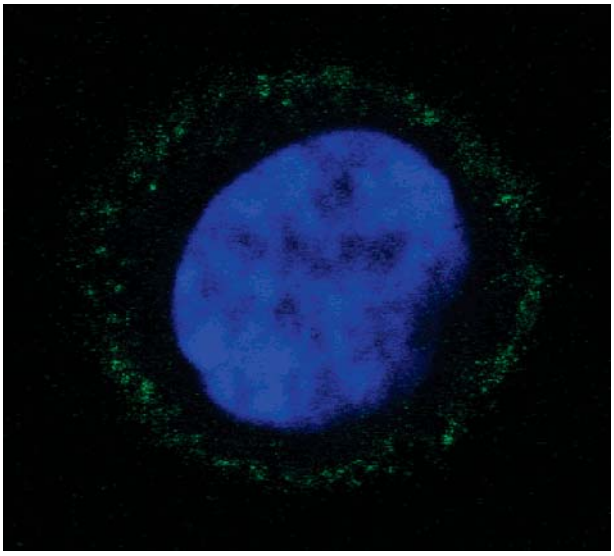

FIGURE 5: Localization of RLIP76 on the cell surface. For cell surface localization of RLIP76 in H358 NSCLC, cells were grown on glass coverslips and live, unfixed cells were subjected to immunohistochemistry utilizing anti-RLIP76 IgG as the primary antibody and FITC-conjugated goat anti-rabbit IgG as the secondary antibody. DAPI was used as a nuclear counterstain. Slides were analyzed using a Zeiss LSM 510META laser scanning fluorescence microscope.

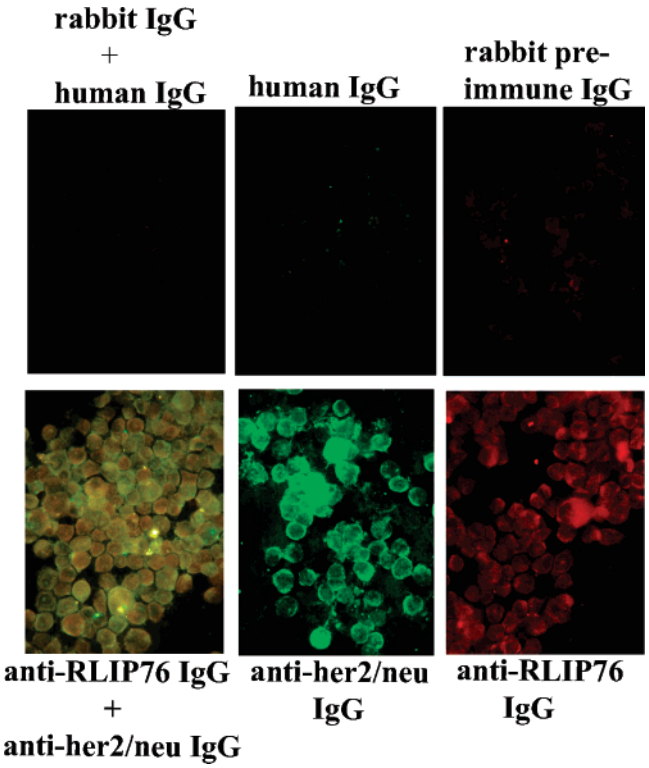

FIGURE 6: Membrane localization of RLIP76. Colocalization of RLIP76 with another protein her2/neu, known to have a cell surface domain. The anti-RLIP76 antibody was detected using a rhodamine red-x-conjugated secondary antibody and an anti-her2/neu antibody using an FITC-tagged secondary antibody. Cell surface epitopes were recognized by both anti-RLIP76 (red fluorescence) and her2/neu antibodies (green fluorescence), and these epitopes colocalized (yellow fluorescence) in unfixed cells, indicating that, like her2/neu, RLIP76 had cell surface epitope(s).

6) and her2/neu antibodies (green fluorescence, Figure 6), and these epitopes colocalized (yellow fluorescence, Figure 6) in unfixed cells, indicating that, like her2/neu, RLIP76 had cell surface epitope(s).

Cell Surface Localization of aa 171−185. Because of the presence of constitutive wild-type RLIP76, H358 cells transfected with the deletion mutants must contain the wild-type and mutant protein in the cell. To examine the effect of only the deletion mutant, we treated cells with siRNA directed at the region encoding aa 171−185, to silence the expression of wild-type RLIP76, while leaving the expression of the aa 171−185 mutant unaffected. Appropriate control siRNA was used in these experiments as detailed in Experimental Procedures. Western blot analyses of cell homogenates treated with either control or experimental siRNA are shown (Figure 7A,B). siRNA aa 171−185 effectively silenced wild-type RLIP76 expression in the untransfected, empty vector-transfected, or wild-type RLIP76-transfected cells as indicated by results showing the failure of the antibodies against peptide 171−185 to detect RLIP76 antigen (Figure 7B). On the other hand, as predicted the antibodies against full-length RLIP76 recognized the persistent presence of the residual deletion mutant RLIP76 (Figure 7A). However, Western blotting against the anti-del171−185 antibody showed no signal in the cells transfected with the RLIP76 deletion mutant (Figure 7B). Together, these results confirmed that the expression of wild-type RLIP76 was effectively blocked in these cells. After establishing that del171−185 could be expressed exclusively in del171−185 overexpressing cells after silencing wild-type RLIP76, we compared the cell surface expression of RLIP76 in del171−185-transfected cells without or with pretreatment with siRNA directed at aa 171−185. Immunohistochemistry was performed using the anti-del171−185 antibody. Results of these studies showed that the cells with control siRNA had a significant cell surface signal consistent with the studies described above (Figure 7C). However, this signal almost completely disappeared in cells upon silencing the expression of wild-type RLIP76 with siRNA (Figure 7D). In aggregate, these studies clearly demonstrate that RLIP76 is an integral membrane protein, and it has at least one cell surface domain spanning the region of aa 171−185.

DISCUSSION

Identifying RLIP76 as a multifunctional protein involved in transport of amphiphilic chemotherapeutic drugs and GS−E (*1*, *2*, *10*−*19*) as well as in signaling pathways (*4*, *9*, *22*−*25*) raises an important question about the subcellular distribution of this protein. In particular, the question about the nature of its association with membranes is intriguing because of the lack of classical transmembrane domains in its primary structure. In the absence of high-resolution three-dimensional structure information for RLIP76, the identification of the domains crucial for its functionality has relied on biochemical and genetic analyses (*4*, *9*, *22*−*25*). Despite the lack of identifiable membrane-spanning domains, there is compelling evidence for the localization of RLIP76, at least partly, in membranes. Its functions in signaling cascades (*4*, *9*, *22*−*25*) strongly suggest its association with the membrane. Likewise, membrane association is a prerequisite for its transport function (*1*, *10*−*19*). It is to be noted DNP-SG ATPase, a transport protein whose identity has now been established with RLIP76, was characterized and isolated from the human erythrocyte membrane vesicles free of cytosol

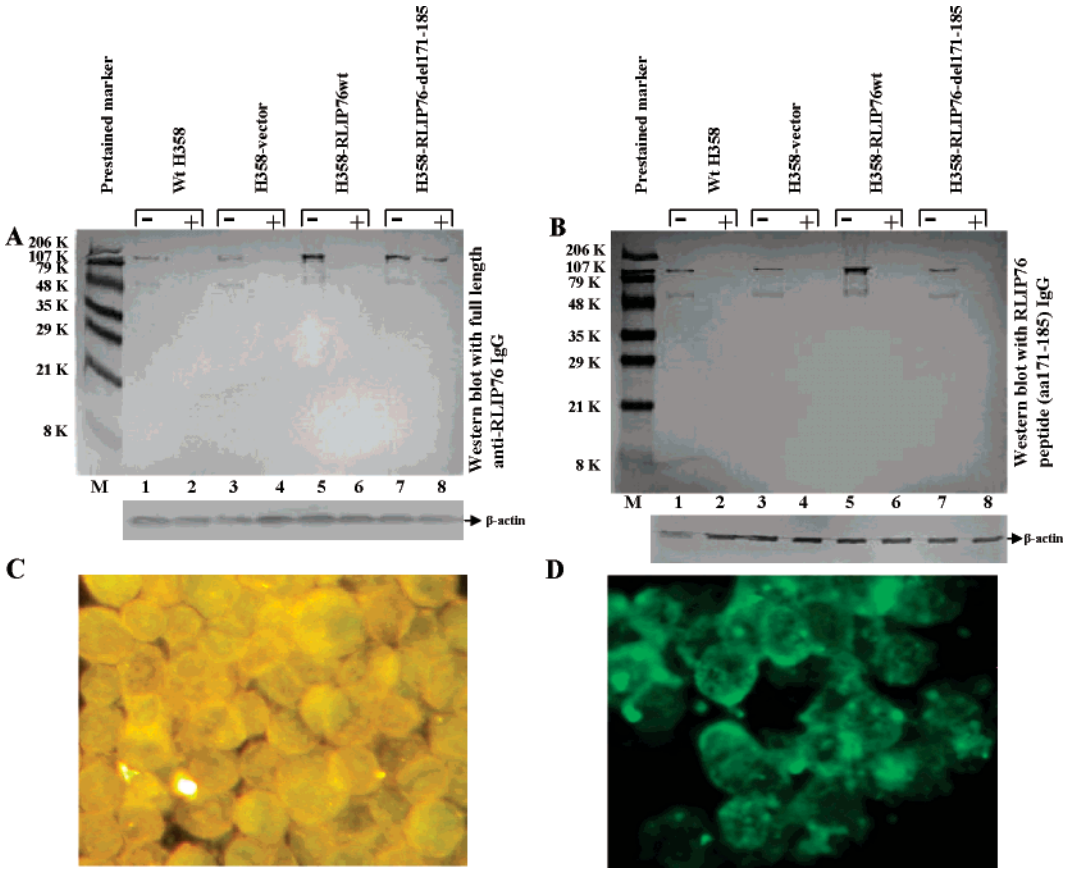

FIGURE 7: Effect of RLIP76 siRNA on protein expression. The protein (100 μg each) from the aliquots of cells was analyzed by Western blot analyses using full-length anti-RLIP76 antibodies (A) and RLIP76 peptide 171−185 antibodies (B): lane M, protein mass markers; lanes 1 and 2, protein from control H358 cells and cells treated with siRNA, respectively; lanes 3 and 4, protein from vector-transfected H358 cells and cells treated with siRNA, respectively; lanes 5 and 6, protein from full-length RLIP76-transfected H358 cells and transfected cells treated with siRNA, respectively; and lanes 7 and 8, protein from del171−185 RLIP76-transfected H358 cells and cells treated with siRNA, respectively. β-Actin expression was used as an internal control. Immunohistochemical localization was performed with H358 cells transfected with del171−185 using both anti-del171−185-RLIP76 IgG and anti-her2/neu IgG. Panel C shows the cells treated with control scrambled siRNA, and panel D shows the cells treated with RLIP76 siRNA. Rhodamine red-x-conjugated goat anti-rabbit IgG and FITC-conjugated goat anti-human IgG were used as secondary antibodies for RLIP76 and her2/neu antibodies, respectively.

(*15*−*18*, *21*). The majority of RLIP76 in eukaryotes as well as in transformed *E. coli* is found associated with the membrane fraction, which can only be extracted by the nonionic detergent (*13*, *14*). We have presented the experimental evidence showing that RLIP76 reconstituted in artificial liposomes is necessary and sufficient for ATP-dependent transport of amphiphilic chemotherapeutic agents as well as GS−E (*11*−*15*). The rat and mouse homologues of RLIP76 (RalBP1 and RIP1, respectively) have also been clearly shown to be membrane-associated in our studies as well in studies by other investigators (*1*, *7*, *8*, *29*−*31*).

Previous studies strongly suggest the presence of RLIP76 epitope(s) on the cell surface. Its localization on the cell surface has been shown by using the highly specific anti-RLIP76 IgG, which blocks the DOX transport in crude vesicles and also inhibits the transport function of RLIP76 in intact cells (*12*, *16*). Flow cytometry studies also suggest that a significant percentage of cells can be detected by anti-RLIP76 IgG, indicating that some domain(s) of RLIP76 recognized by these specific antibodies is present at the cell surface (*12*). Additional evidence for the localization of RLIP76 on the surface of the cell comes from the immunohistochemistry studies that suggest localization of RLIP76 on the plasma membrane and nuclear envelope (*12*, *20*).

These studies aimed to identify the cell surface domain of RLIP76 and to determine the role in transport function of RLIP76. We systematically made a series of deletion mutants to identify domains and residues implicated in membrane anchoring to examine how these hydrophobic regions affect membrane association and the transport properties of RLIP76. Sequence alignment (Figure 1) shows that RLIP76 has several sequences homologous with those of cell-penetrating peptides such as penetratin, TAT, MAP, and transportan (*37*, *38*). The region corresponding to aa 154−170 is rich in lysine residues which may interact with the negatively charged phospholipid membranes. The region corresponding to aa 203−219 is the region of high hydrophobicity; therefore, it is a suitable candidate for spanning the membrane and aa 171−185 region which is rich in proline, and isoleucine makes it a suitable candidate for being on the surface of the membrane. It has been shown in vector peptides that the peptide helicity plays no decisive role in peptide translocation in the membranes and that the amphiphilicity of the peptide is much more important. Penetratin peptides interact with the cell membrane presumably with the electrostatic forces between the positively charged Arg/Lys and negatively charged phospholipids. Another important interaction includes the apolar interaction between hydrophobic side chains

and the apolar part of the lipid bilayer. Since suitably specific antibodies could not be raised against the entire peptide encompassing aa 154−219, our findings leave open the possibility that the cell surface domain is not limited only to aa 171−185. Likewise, because membrane association could not be completely abrogated by deleting aa 154−219, it is likely that other regions may also be involved in mediating membrane anchoring of RLIP76.

The results of these studies show that deletion of aa 154−219 markedly inhibits its membrane association and, consequently, its transport activity toward anionic allocrite DNP-SG as well as amphiphilic weakly cationic allocrite DOX. Membrane association of a transporter is a prerequisite for its function, and these studies for the first time show a correlation between membrane localization and transport activity of RLIP76. Our immunohistochemical studies using both confocal laser microscopy and conventional microscopy demonstrated cell surface localization of RLIP76 and identified cell surface epitopes. The lack of immunohistochemical deletion of RLIP76 on the surface of cells which selectively express the deletion mutant aa 171−185 (expression of wt-RLIP76 was silenced in these cells with aa 171−185 siRNA) provides strong evidence that aa 171−185 are a part of a cell surface domain of RLIP76. Our data for partitioning of various deletion mutants with membrane and cytosolic fractions and the transport activity of these mutants also strongly suggest that aa 171−185 make up one of the cell surface epitopes and the region of aa 154−219 in general is a determinant of its transport function.

We have also demonstrated that deletion of the ATP-binding sites does not affect membrane association of RLIP76 but completely abrogates its transport activity. These results further confirm our previous conclusions that ATP hydrolysis is coupled with RLIP76-mediated efflux of DOX as well as DNP-SG. It is to be noted that the deletion of aa 154−219 or 171−185 results in the loss of only approximately half of the transport activity of RLIP76 with a concomitant decrease in its level of membrane association. Residual transport activity of the aa 154−219 deletion mutant suggests that additional sequences within RLIP76 may also contribute to its membrane association and consequently its transport function. While further studies are required to identify the presence of any membrane-associated regions, the results presented in this communication clearly demonstrate that aa 154−219 are determinants for its anchoring to the membrane and its ATP-dependent transport of anionic as well as amphiphilic drugs. It is likely that in the absence of the classical transmembrane domains, certain physicochemical properties of these domains (e.g., positive charge, hydrophobicity, and amphipathicity) may govern them to associate with the lipid membrane. Further studies are needed to elucidate the nature of these associations.

REFERENCES

1. Awasthi, S., Singhal, S. S., Sharma, R., Zimniak, P., and Awasthi, Y. C. (2003) Transport of glutathione-conjugates and chemotherapeutic drugs by RLIP76 (RALBP1): A novel link between G-protein and tyrosine kinase signaling and drug resistance, *Int. J. Cancer 106*, 635−646.
2. Yang, Y., Sharma, A., Sharma, R., Patrick, B., Singhal, S. S., Zimniak, P., Awasthi, S., and Awasthi, Y. C. (2003) Cells preconditioned with mild, transient UVA irradiation acquire resistance to oxidative stress and UVA-induced apoptosis: Role of 4-hydroxynonenal in UVA-mediated signaling for apoptosis, *J. Biol. Chem. 278*, 41380−41388.
3. Jullien-Flores, V., Dorseuil, O., Romero, F., Letourneur, F., Saragosti, S., Berger, R., Tavitian, A., Gacon, G., Camonis, J. H., and Cool, R. H. (1995) Bridging Ral GTPase to Rho pathways. RLIP76, a Ral effector with CDC42/Rac GTPse-activating protein activity, *J. Biol. Chem. 270*, 22473−22477.
4. Rosse, C., L'Hoste, S., Offner, N., Picard, A., and Camonis, J. H. (2003) RLIP, an effector of the Ral GTPases, is a platform for cdk1 to phosphorylate epsin during the switch off of endocytosis in mitosis, *J. Biol. Chem. 278*, 30597−30604.
5. Wolthuis, R. M., Franke, B., van Triest, M., Bauer, B., Cool, R. H., Camonis, J. H., Akkerman, J. W., and Bos, J. L. (1998) Activation of the small GTPase Ral in platelets, *Mol. Cell. Biol. 18*, 2486−2491.
6. Bauer, B., Mirey, G., Vetter, I. R., Garcia-Ranea, J. A., Valencia, A., Wittinghofer, A., Camonis, J. H., and Cool, R. H. (1999) Effector recognition by the small GTP-binding proteins Ras and Ral, *J. Biol. Chem. 274*, 17763−17770.
7. Park, S. H., and Weinberg, R. A. (1995) A putative effector of Ral has homology to Rho/Rac GTPase activating proteins, *Oncogene 11*, 2349−2355.
8. Cantor, S. B., Urano, T., and Feig, L. A. (1995) Identification and Characterization of Ral-binding protein 1, a potential downstream target of Ral GTPases, *Mol. Cell. Biol. 15*, 4578−4584.
9. Ikeda, M., Ishida, O., Hinoi, T., Kishida, S., and Kikuchi, A. (1998) Identification and characterization of a novel protein interacting with Ral-binding protein 1, a putative effector protein of Ral, *J. Biol. Chem. 273*, 814−821.
10. Singhal, S. S., Singhal, J., Sharma, R., Singh, S. V., Zimniak, P., Awasthi, Y. C., and Awasthi, S. (2003) Role of RLIP76 in lung cancer doxorubicin resistance I. The ATPse activity of RLIP76 correlates with doxorubicin and 4-hydroxynonenal resistance in lung cancer cells, *Int. J. Oncol. 22*, 365−375.
11. Awasthi, S., Singhal, S. S., Singhal, J., Cheng, J., Zimniak, P., and Awasthi, Y. C. (2003) Role of RLIP76 in lung cancer doxorubicin resistance II. Doxorubicin transport in lung cancer by RLIP76, *Int. J. Oncol. 22*, 713−720.
12. Awasthi, S., Singhal, S. S., Singhal, J., Yang, Y., Zimniak, P., and Awasthi, Y. C. (2003) Role of RLIP76 in lung cancer doxorubicin resistance III. Anti-RLIP76 antibodies trigger apoptosis in lung cancer cells and synergistically increase doxorubicin cytotoxicity, *Int. J. Oncol. 22*, 721−732.
13. Awasthi, S., Cheng, J., Singhal, S. S., Saini, M. K., Pandya, U., Pikula, S., Bandorowicz-Pikula, J., Singh, S. V., Zimniak, P., and Awasthi, Y. C. (2000) Novel function of human RLIP76: ATP-dependent transport of glutathione conjugates and doxorubicin, *Biochemistry 39*, 9327−9334.
14. Awasthi, S., Cheng, J. Z., Singhal, S. S., Pandya, U., Sharma, R., Singh, S. V., Zimniak, P., and Awasthi, Y. C. (2001) Functional reassembly of ATP-dependent xenobiotics transport by the N-and C-terminal domains of RLIP76 and identification of ATP binding sequence, *Biochemistry 40*, 4159−4168.
15. Awasthi, S., Singhal, S. S., Srivastava, S. K., Zimniak, P., Bajpei, K. K., Saxena, M., Sharma, R., Ziller, S. A., Frenkel, E. P., Singh, S. V., He, N. G., and Awasthi, Y. C. (1994) Adenosine triphosphate-dependent transport of doxorubicin, daunomycin and vinblastine in human tissues by a mechanism distinct from the P-glycoprotein, *J. Clin. Invest. 93*, 958−965.
16. Cheng, J. Z., Sharma, R., Yang, Y., Singhal, S. S., Sharma, A., Saini, M. K., Singh, S. V., Zimniak, P., Awasthi, S., and Awasthi, Y. C. (2001) Accelerated metabolism and exclusion of 4-hydroxynonenal through induction of RLIP76 and hGST5.8 is an early adaptive response of cells to heat and oxidative stress, *J. Biol. Chem. 276*, 41213−41223.
17. Awasthi, S., Singhal, S. S., Srivastava, S. K., Torman, R. T., Zimniak, P., Bandorowicz-Pikula, J., Singh, S. V., Piper, J. T., Awasthi, Y. C., and Pikula, S. (1998) ATP-dependent human erythrocyte glutathione-conjugate transporter I. Purification, photoaffinity labeling, and kinetics characteristics of ATPase activity, *Biochemistry 37*, 5231−5238.
18. Awasthi, S., Singhal, S. S., Pikula, S., Srivastava, S. K., Torman, R. T., Bandorowicz-Pikula, J., Lin, J. T., Singh, S. V., Zimniak, P., and Awasthi, Y. C. (1998) ATP-dependent human erythrocyte glutathione-conjugate transporter II. Functional reconstitution of transport activity, *Biochemistry 37*, 5239−5248.

19. Awasthi, S., Sharma, R., Singhal, S. S., Zimniak, P., and Awasthi, Y. C. (2002) RLIP76, a novel transporter catalyzing ATP-dependent efflux of xenobiotics, *Drug Metab. Dispos. 30*, 1300−1310.
20. Awasthi, S., Sharma, R., Yang, Y., Singhal, S. S., Pikula, J., Singh, S. V., Zimniak, P., and Awasthi, Y. C. (2002) Transport functions and physiological significance of 76 kDa Ral-binding GTPase activating protein (RLIP76), *Acta Biochim. Pol. 49*, 855−867.
21. Sharma, R., Singhal, S. S., Cheng, J., Yang, Y., Sharma, A., Zimniak, P., Awasthi, S., and Awasthi, Y. C. (2001) RLIP76 is the major ATP-dependent transporter of glutathione-conjugates and doxorubicin in human erythrocytes, *Arch. Biochem. Biophys. 391*, 171−179.
22. Kariya, K., Koyama, S., Nakashima, S., Oshiro, T., Morinaka, K., and Kikuchi, A. (2000) Regulation of complex formation of POB1/epsin/adaptor protein complex 2 by mitotic phosphorylation, *J. Biol. Chem. 275*, 18399−18406.
23. Quaroni, A., and Paul, E. C. (1999) Cytocentrin is a Ral-binding protein involved in the assembly and function of the mitotic apparatus, *J. Cell Sci. 112*, 707−718.
24. Matsuzaki, T., Matsuzaki, T., Hanai, S., Kishi, H., Liu, Z., Bao, Y., Kikuchi, A., Tsuchida, K., and Sugino, H. (2002) Regulation of endocytosis of activin type II receptors by a novel PDZ protein through Ral/Ral-binding protein 1-dependent pathway, *J. Biol. Chem. 277*, 19008−19018.
25. Moskalenko, S., Henry, D. O., Rosse, C., Mirey, G., Camonis, J. H., and White, M. A. (2002) The exocyst is a Ral effector complex, *Nat. Cell Biol. 4*, 66−72.
26. Sharma, R., Singhal, S. S., Wickramarachchi, D., Awasthi, Y. C., and Awasthi S. (2004) RLIP76 (RALBP1) mediated transport of leukotriene C4 (LTC4) in cancer cells: Implications in drug-resistance, *Int. J. Cancer 112*, 934−942.
27. Matsubara, K., Hinoi, T., Koyama, S., and Kikuchi, A. (1997) Post-translational modifications of Ral and Rac1 are important for the action of Ral-binding protein 1, a putative effector protein of Ral, *FEBS Lett. 410*, 169−174.
28. Oosterhoff, J., Penninkhof, K. F., Brinkmann, A. O., Grootegoed, J. A., and Blok, L. J. (2003) REPS2/POB1 is downregulated during human prostate cancer progression and inhibits growth factor signaling in prostate cancer cells, *Oncogene 22*, 2920−2925.
29. Swatko, M. E., Cheng, J. Z., Singhal, S. S., Awasthi, Y. C., Awasthi, S., and Zimniak, P. (2001) Rat RalBP1 is an ATP-dependent transporter of organic anions, *Chem.-Biol. Interact. 133*, 249−255.
30. Pikula, S., Hayden, J. B., Awasthi, S., Awasthi, Y. C., and Zimniak, P. (1994) Organic anion-transporting ATPase of rat liver. I. Purification, photoaffinity labeling, and regulation by phosphorylation, *J. Biol. Chem. 269*, 27566−27573.
31. Pikula, S., Hayden, J. B., Awasthi, S., Awasthi, Y. C., and Zimniak, P. (1994) Organic anion-transporting ATPase of rat liver. II. Functional reconstitution of active transport and regulation by phosphorylation, *J. Biol. Chem. 269*, 27574−27579.
32. Drin, G., Cottin, S., Blanc, E., Rees, A. R., and Temsamani, J. (2003) Studies on the internalization mechanism of cationic cell-penetrating peptides, *J. Biol. Chem. 278*, 31192−31201.
33. Letoha, T., Gaal, S., Somlai, A., Czajlik, A., Perczel, A., and Penke, B. (2003) Membrane translocation of penetratin and its derivatives in different cell lines, *J. Mol. Recognit. 16*, 272−279.
34. Sambrook, J., Fritsch, E. F., and Miniatis, T. (1989) *Molecular Cloning: A laboratory manual*, 2nd ed., Cold Spring Harbor Laboratory Press, Plainview, NY.
35. Minamide, L. S., and Bamburg, J. R. (1990) A filter paper dye-binding assay for quantitative determination of protein without interference from reducing agents or detergents, *Anal. Biochem. 190*, 66−70.
36. Towbin, H., Staehelin, T., and Gordon, J. (1979) Electrophoretic transfer of protein from polyacrylamide gels to nitrocellulose sheets: Procedure and some applications, *Proc. Natl. Acad. Sci. U.S.A. 76*, 4350−4353.
37. Richard, J. P., Melikov, K., Vives, E., Ramos, C., Verbeure, B., Gait, M. J., Chernomordik, L. V., and Lebleu, B. (2003) Cell-penetrating peptides: A reevaluation of mechanism of cellular uptake, *J. Biol. Chem. 278*, 585−590.
38. Drin, G., Delene, H., Temsamani, J., and Brasseur, R. (2001) Translocation of the pAntp peptide and its amphipathic analogue AP-2AL, *Biochemistry 40*, 1824−1834.

BI0482811